European Journal of Medicinal Chemistry 46 (2011) 1779–1788

Contents lists available at ScienceDirect

European Journal of Medicinal Chemistry

journal homepage: http://www.elsevier.com/locate/ejmech

Original article

Synthesis, in vitro screening and in vivo evaluation of cyclic RGD analogs cyclized through oxorhenium and oxotechnetium coordination

Marie Aufort, Marta Gonera [1], Marie-Anne Lelait [1], Bertrand Czarny, Loïc Le Clainche, Robert Thaï, Amandine Landra, Mathias Ruinart de Brimont, Christophe Dugave*

CEA/Saclay, iBiTec-S/SIMOPRO, Bâtiment 152, 91191 Gif-sur-Yvette, France

ARTICLE INFO

Article history:
Received 25 November 2010
Received in revised form
10 February 2011
Accepted 11 February 2011
Available online 22 February 2011

Keywords:
Integrin
RGD
Angiogenesis
Rhenium
Technetium
Cyclopeptide

ABSTRACT

A library of RGD tripeptide analogs cyclized through oxorhenium coordination by an NS_2/S chelation motif was synthesized. Screening towards integrins αVβ3, αIIbβ3 and αVβ5 led to the identification of 6 oxorhenium complexes that bind to integrin αVβ3 in the submicromolar range. *In vivo* evaluation of five of the corresponding oxotechnetium complexes using nude mice bearing a U87MG human tumor xenograft showed a significant and specific accumulation of radioactivity inside the tumor. The best results *in vivo* were obtained with complexes **Tc-16** and **Tc-50** that displayed a higher tumor accumulation and a lower distribution in other tissues relative to a reference cyclopentapeptide tracer.

1. Introduction

The family of heterodimeric integral glycoproteins integrins plays a central role in cell-adhesion and cell–matrix interaction and is consequently implicated in a number of biological processes as well as several diseases [1]. In particular, integrin αVβ3 is involved in neoangiogenesis and actively participates in the control of cancer development and metastatic processes [2]. Several integrins, in particular αVβ3, have been validated as markers of cancer progression [3,4] and hence are the targets of numerous antagonists that have been proposed as anti-neoangiogenic agents [5].

Eight of the 24 known integrins specifically recognize a structured RGD sequence in endogenous ligands the conformation of which orientates integrin selectivity [6,7]. A huge number of RGD-based integrin antagonists have been reported in the literature, including cyclic and acyclic compounds [8,9]. To date, Cilengitide® **1** (Fig. 1), one of the more promising integrin αVβ3 antagonist [10], and analogs **2** and **3** have inspired a variety of neoangionenesis-directed tracers [11–16]. In particular, cyclopentapeptides **5** and **6** have been widely used for *in vivo* tumor imaging using ^{18}F [17,18,22], ^{64}Cu [20,23,24], ^{99m}Tc [13,25–31], ^{111}In [14,32] and ^{125}I-labeled [33–35] bioconjugates (see labeled compounds **7**–**15** in the Supplementary Material section).

Although most of these tracers have been developed using the bifunctional chelating agent (BFCA) approach that conjugates an integrin-specific moiety to a labeled pending motif, some other strategies have been explored [36,37]. In particular, we were interested in the development of new Tc/Re-essential integrin antagonists [38]. In these complexes, technetium (or its chemical analog rhenium) plays an additional structural role that therefore contributes to orientate amino acids side-chains. This approach was successfully applied to the development of Tc/Re cyclized analogs of various bioactive peptides such as α-melanotropin [39,40] human neutrophil elastase inhibitors [37], α-MSH [41], GnRH [42], somatostatin [43,44] and adrenomedullin [45] as well as RGD peptides [46]. We previously reported the design and synthesis of a cyclic cyclophilin oxorhenium inhibitor that contains an NS_2/S motif which unambiguously coordinates the oxometal core [47]. We also recently investigated the development of a new integrin antagonist **Re-16** cyclized through oxorhenium/oxotechnetium coordination by the NS_2/S chelation motif. This compound contains a canonic RGD sequence linked to a *N*-bis(2-thioethyl)glycine moiety (called NS_2-motif) at the N-terminus and a 2-aminoethanethiol C-terminus that cooperate together to chelate the oxometal core (Scheme 1). Compound **Re-16** exhibited an IC_{50} of 86 nM for integrin αVβ3 and a lower affinity for integrin αIIbβ3 ($IC_{50} = 1120$ nM) [38]. We planned

* Corresponding author. Tel.: +33 16908 5225; fax: +33 16908 9071.
E-mail address: christophe.dugave@cea.fr (C. Dugave).
[1] These two authors have performed equivalent contributions to this work.

0223-5234/$ – see front matter © 2011 Elsevier Masson SAS. All rights reserved.
doi:10.1016/j.ejmech.2011.02.032

Abbreviations

b	broad
Boc	tert-butyloxycarbonyl
Dab	2,4-diaminobutyric acid
DCC	dicyclohexylcarbodiimide
DIPEA	di-iso-propylethylamine
DMSO	dimthylsulfoxide
Dpr	2,3-diaminopropionic acid
EMEM	Eagle's minimum essential medium
Fmoc	fluorenylmethoxycarbonyl
GnRH	gonadotropin-releasing hormone
HATU	2-(1H-7-azabenzotriazol-1-yl)-1,1,3,3-tetramethyl uronium hexafluoro-phosphate methanaminium
HEPES	4-(2-hydroxyethyl)-1-piperazineethanesulfonic acid
HOBT	N-hydroxybenzotriazole
HRMS	high-resolution mass spectrometry
ID/g	percentage of injected dose per gram of tissue
ivDde	1-(4,4-dimethyl-2,6-dioxo-cyclohexylidene)-3-methyl-butyl
LC–ESMS	liquid chromatography coupled to electrospray mass spectrometry
m	multiplet
Mmt	4-methoxytrityl
NMR	nuclear magnetic resonance
NS_2/S	N-bis(2-thioethyl)glycine/thiol chelation motif
Pbf	2,2,4,6,7-pentamethyl-dihydrobenzofurane-5-sulfonyl
PEG-PS	polyethyleneglycol-polystyrene resin
RP-HPLC	reverse phase high performance liquid chromatography
s	singlet
SPPS	solid phase peptide synthesis
tBu	tert-butyl
t triplet T/B	tumor/blood radioactivity ratio
T/M	tumor/muscles radioactivity ratio
TFA	trifluoroacetic acid
TIPS	tri-iso-propylsilane
Tr	trityl
α-MSH	α-melanocyte stimulating hormone
β	β-alanine

to investigate the potential of such a complex as tracer for the molecular imaging of cancer using nude mice bearing a human tumor xenograft model U87MG which mainly overexpresses integrin αVβ3 [17,21–24]. For this purpose, we decided to test series of **Re-16** analogs with various side-chain lengths, absolute configurations and C-terminal linkers. Starting from compound **Re-16**, we developed a small library of complexes that contains all possible combinations of D/L-Arg (including homologs), Gly/β-Ala and D/L-Asp or Glu residues, and a variable C-terminal thiol (2 aliphatic and 3 aromatic amino-thiols). Moreover, existence of multiple isomerisms around the oxometal core was anticipated to lead to four possible isomers from a single starting peptide and to increase the structural diversity of the library of complexes [38,47–51].

In this paper, we describe the parallel resin-supported synthesis of 86 modified peptides, their complexation with the oxorhenium core and the screening of the corresponding rhenium complexes towards integrins αVβ3, αIIbβ3 and αVβ5. Technetium labeling, stability studies and *in vivo* evaluation of the 'hit complexes' are also reported. All data are compared to tracer **Tc-14** [19] which has been studied in the same conditions as a reference compound.

2. Results and discussion

2.1. Design rationale

Informative data should be obtained from the structure resolution of complex **Re-16** that has displayed an interesting activity towards integrins. In particular, preliminary results obtained *in vitro* with this compound strongly suggested that only one of the two diastereomers binds to integrin αVβ3 [38]. As previously reported, the conformational plasticity of [NS_2–ReO–S] complexes that enables a spontaneous interconversion of diastereomers [47–51] precluded durable isomer separation and crystallization. This phenomenon also putatively prevented the accurate resolution of structure by two-dimensional high-field NMR spectrometry. In the

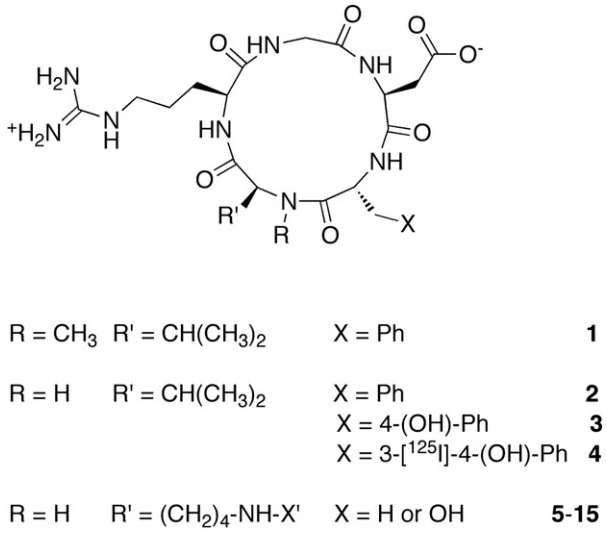

Fig. 1. Structures of cyclic antagonists of integrin αVβ3 **1**–**3** and their derived tracers **4**–**15**: X′ is either a propionyl group (compound **7**) a [^{18}F] fluorinated moiety (compounds **8** and **9**) or a BFCA (compounds **10**–**15**).

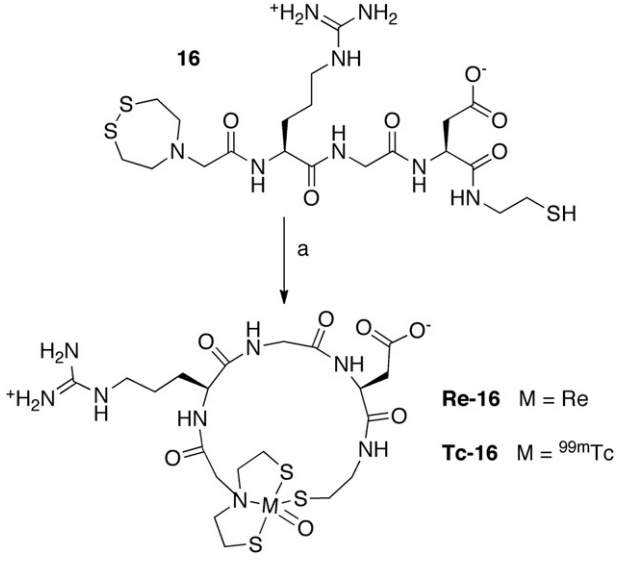

Scheme 1. Cyclization of peptide **16** to the corresponding oxorhenium or oxotechnetium complex **M-16** (M = Re or ^{99m}Tc). a: $Bu_4NReOCl_4$, DIPEA in methanol or $Na^{99m}TcO_4$, $SnCl_2$, sodium gluconate.

absence of validated simulation methods that enable the prediction of structure of oxotechnetium and oxorhenium complexes, *in silico* design of Tc/Re-containing integrin ligands was difficult, despite the existence of pharmacophoric models proposed for several integrin antagonists [8,52,53]. Therefore, we preferred a combinatorial approach based on a general model to access to a representative chemical diversity of potential integrins ligands.

Our model compound was complex **Re-16** that features a 13-bond distance between the guanidinium and carboxylate carbons. This distance was equivalent to that observed in cyclopentapeptides **1**–**6** (13 bonds) that preferentially bind to integrin αVβ3 [54] as well as in most non-peptide integrin antagonists [9]. Therefore, we investigated the effect of absolute configuration inversion at the different positions as well as cycle constraint and relaxation using various C-terminal motifs combined with variations of side-chain length at S1 and S3 (Figs. 2 and 3). We limited the guanidinium–carboxylate 'distance' between 11 and 15 bonds throughout this study. Side-chains length variations as well as β-Ala/Gly substitutions were expected to modify the guanidinium–carboxylate distance while amino acids absolute configuration and modifications at C-terminus either increase or relax cycle constraints that also might affect side-chains distances and positioning (Table 1).

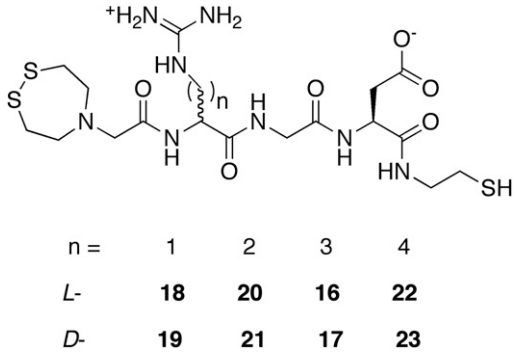

Fig. 3. Sequences and numbering of homolog peptides of compounds **16** and their epimers at S1.

2.2. Peptide synthesis

In our previous paper, we used a (Fmoc-Asp(γ-PEG-PS)-allyl) resin to synthesize peptide **16**. In order to avoid the use of expensive and highly sensitive tetrakis(triphenylphosphine)palladium(0) employed to remove the allyl group selectively, we investigated a new synthetic route that uses a methoxytrityl (Mmt) resin grafted with various C-terminal thioalkyl/thioaryl amines through an acid-sensitive trityl-thiol moiety (see Supporting Material section). The 2-aminoethanethiol-chloromethoxytrityl (Mmt) resin was available commercially. Sets of batches of resin grafted, respectively, with 3-aminopropanethiol, 2-, 3- and 4-aminothiophenol were prepared as follows: commercial chloromethoxytrityl resin (Cl-Mmt) was treated with the aminothiol and di-*iso*-propylethylamine to give the corresponding trityl-thiol adduct that serves as protecting group and resin linking motif concurrently. Loading yields, determined by quantitative Kaiser test, typically reached 90% except in the case of 3-aminopropanethiol (19%) which required the amine to be protected with a Fmoc group prior to grafting. Moreover, 3-aminopropanethiol should be synthesized starting from 3-aminopropanol using classical chemical procedures.

The first amino acid was coupled on to the linker using HATU as coupling reagent. Peptide elongation was carried out by standard Fmoc-solid phase peptide synthesis (Fmoc-SPPS) procedure using DCC and HOBT. The NS_2 moiety, synthesized as previously reported [38] was grafted on to the peptide N-terminus by HATU-mediated coupling. Peptide deprotection and cleavage from the resin were carried out in a mixture of TFA and scavengers (water and tri-*iso*-propylsilane) followed by HPLC purification that enabled to isolate the peptides with satisfactory purities (typically >95% as assessed by LC–ES/MS analysis). In some cases, peptides tend to dimerize spontaneously by thiol oxidation of the S moiety during further handling and storage. Both reduced and oxidized forms were separated during purification.

Peptide **16** analogs containing arginine homologs were synthesized from the corresponding commercially available diamino acids as depicted in Scheme 3 in Supporting Material, except peptide **17** which was obtained from Fmoc-D-Arg(Pbf)-OH by the procedure described above. Fmoc-2,3-diaminopropionate, Fmoc-2,4-diaminobutyrate and Fmoc-lysine protected with an ivDde group on the side-chain amine were used as precursors of arginine homologs. Selective ivDde removal with hydrazine followed by reaction of the free amine with di-Boc-1H-pyrazole-1-carboxamidine and final deprotection/cleavage steps gave peptides **18**–**23** (Fig. 3).

Peptides **16**–**85** were isolated and their structures were confirmed by ^{1}H and ^{13}C NMR and ES/MS spectroscopy analysis

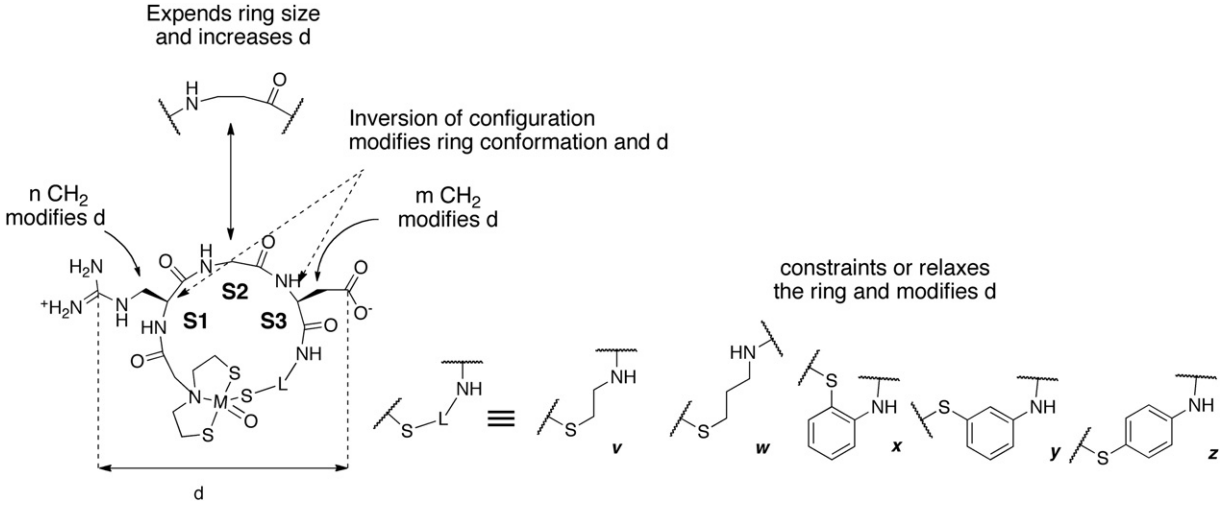

Fig. 2. Expected effects on distance *d*, ring size and ring conformation of sequential and combined modifications of the lead compound **Re-16** ($n = 3$, $m = 1$, 1-*L*,3-*L*) obtained through either oxorhenium (M = Re) or oxotechnetium (M = ^{99m}Tc) complexation by the corresponding NS_2/S peptide.

Table 1
Sequence and corresponding numbering of peptides (v: 2-aminoethanethiol; w: 3-aminopropanethiol; x: 2-aminothiophenol; y: 3-aminothiophenol; z: 4-aminothiophenol, β: β-alanine).

Tripeptide sequence																C-terminus
RGD	RBD	RGE	RβE	rGd	rβd	rGe	rβe	RGd	Rβd	RGe	Rβe	rGD	rβD	rGE	rβE	
16	**24**	**25**	**26**	**27**	**28**	**29**	**30**	**31**	**32**	**33**	**34**	**17**	**35**	**36**	**37**	v
38	**39**	**40**	**41**	**42**	**43**	**44**	**45**	**46**	**47**	**48**	**49**	**50**	**51**	**52**	**53**	w
–[a]	–[a]	–[a]	–[a]	–[a]	–[a]	–[a]	–[a]	–[a]	–[a]	–[a]	–[a]	–[a]	–[a]	–[a]	–[a]	x
54	**55**	**56**	**57**	**58**	**59**	**60**	**61**	**62**	**63**	**64**	**65**	**66**	**67**	**68**	**69**	y
70	**71**	**72**	**73**	**74**	**75**	**76**	**77**	**78**	**79**	**80**	**81**	**82**	**83**	**84**	**85**	z

[a] The peptides in the ortho series were synthesized by parallel SPPS as reported; loading determination and successive Kaiser tests indicated correct coupling reactions however an exclusive C-terminal cyclization into the corresponding imide was observed after the deprotection/cleavage step (see Scheme S4 in Supplementary Material).

except in the 2-aminothiophenol series. As a matter of fact, the corresponding imidic compounds were isolated and unambiguously identified instead of the desired peptide derivatives. These products, formed during peptide deprotection and cleavage, result from the cyclization of the amide into imide. This process might be facilitated by the formation of an internal H-bond that is likely to increase the anilide nucleophilicity in acidic conditions. Such a rearrangement has been reported in the literature for Asp-Gly sequences [55–57] and some examples are also known in the glutamate series [58,59]. In order to clarify this point, we prepared compound **86** which was treated in a mixture of TFA:TIPS:water 95:2.5:2.5 to give the corresponding glutarimide **88** almost exclusively (see Supplementary Material section). All our attempts to synthesize the desired peptides in solution failed and therefore, the preparation of compounds in the *x* series was abandoned.

2.3. Oxorhenium complexation and in vitro screening towards integrins

In a preliminary study, we evaluated the effect of the length of arginine side-chain on the affinity and selectivity for integrins αVβ3, αIIbβ3 and αVβ5. For this purpose we constructed the S1 homologs of peptide **16** [38] and their corresponding epimers **18**–**23** (Fig. 3). These compounds were successfully complexed to the oxorhenium core using commercial tetrabutylammonium tetrachlorooxorhenate in methanol as previously reported [38,47,51]. After precipitation, centrifugation, washing and purification through a Sep-Pak cartridge, the complexes were evaluated as ligands of integrins. The integrin binding assays were carried out as reported in our previous paper [38] using home-made [^{125}I]echistatin as a radio-ligand for competition (Table 2).

We confirmed preliminary results obtained with compound **Re-16** ($IC_{50} = 86$ nM for integrin αVβ3) [38] that exhibited a marked preference for integrin αVβ3 relative to integrins αIIbβ3 and αVβ5. This RGD complex bearing a 2-aminoethanethiol C-terminus has an affinity which is equivalent to that of cyclopentapeptides **2** and **7** (the non-labeled equivalent of tracer **T-7**) that also possesses a constrained RGD sequence. Not surprisingly inversion of the Cα absolute configuration at S1 caused a decrease of the affinity for αVβ3 by one order of magnitude. We also observed that length variation of the arginine alkyl side-chain resulted in a dramatic fall of the affinity compared to the active complex **Re-16** except in the case of **Re-22** and **Re-23** that conserve an affinity for integrin αIIbβ3 in the micromolar range. Considering that substitution of arginine with lower (compounds **18**–**21**) and higher homologs (compounds **22** and **23**) does not provide any improvement of the affinity and implies two supplementary synthetic steps, we decided to limit our investigations to peptides in the D- and L-Arginine series ($n = 3$) as shown in Table 1.

Parallel complexation of oxorhenium by peptides **24**–**85** was performed as reported above. From a set of 64 possible complexes, we only obtained 48 oxorhenium compounds since complexation revealed to be difficult in the 4-aminothiophenol series (Table 1, *z* series): only traces of the corresponding oxorhenium complexes were isolated for peptides **70**–**85**. This result might reflect particular strains inside the complex cycle that would be caused by the extended and rigid C-terminus. As already observed with peptide **16** [38], oxorhenium complexation in the alkyl and aryl meta series (respectively *v*, *w* and *y* C-termini), led to the formation of 2 geometrical isomers in most cases though up to 4 diastereomers were obtained from a single peptide as monitored by LC–ES/MS. These diastereomers result form mutiple *syn*/*anti* isomerisms around the oxorhenium core. Moreover, a small and variable amount of heterodimer was also detected though the monomers were obtained as major products in the experimental conditions used for oxorhenium complexation [38]. The diastereomers were not separated due to the configurational instability of the $[NS_2 \cdot ReO \cdot S]$ asymmetric center that tends to epimerize slowly in buffers as previously observed [38]. In contrast, complexation of $^{99m}TcO^{3+}$ after thiol reduction gave a single isomer (monomer only) in most cases except in the case of peptide **33** that gave two peaks upon ^{99m}Tc complexation (RP-HPLC $t_R = 13.5 + 14.9$ min). These differences between complexation kinetics of the two metal cores lead to distinct mixture compositions. They result: (i) from higher concentrations in oxorhenium that facilitate the preparative synthesis of ReO^{3+} complexes whereas $^{99m}TcO^{3+}$ is obtained in nanomolar concentrations as already observed with complexes **Tc**/**Re-16** [38]; and (ii) from the higher reactivity of technetium relative to rhenium that facilitates metal complexation [60].

Stability studies of a selection of technetium complexes that feature different ring size and absolute configurations at S1 and S3 Cα showed that these compounds exhibit a satisfactory stability after incubation for 6 h in a buffer pH 7.8 in the presence of 1 mM

Table 2
IC_{50} of compounds **16**–**23** (duplicate) and **33**, **50**, **54**, **66** determined using the echistatin competition assay on integrins αVβ3, αIIbβ3 and αVβ5.

Compounds	IC_{50} αVβ3 (μM)	IC_{50} αIIbβ3 (μM)	IC_{50} αVβ5 (μM)
2[a]	0.067 ± 0.035	0.675 ± 0.06	2.1 ± 1
7[b]	0.053 ± 0.005	0.64 ± 0.3	ND
Re-16[a]	0.060 ± 0.012[c]	1.7 ± 0.4	1.1 ± 0.2
Re-17	0.55 ± 0.2	2.4 ± 0.6	1.5 ± 0.9
Re-18	5.6 ± 0.35	>10	>10
Re-19	>10	>10	8.1 ± 1.4
Re-20	1.5 ± 0.3	>10	> 10
Re-21	2.0 ± 0.33	9.1 ± 5	9.1 ± 1.2
Re-22	>10	3.8 ± 1.3	>10
Re-23	>100	2.0 ± 0.3	>10
Re-33	0.47 ± 0.12	0.24 ± 0.06	1.0 ± 0.1
Re-50	0.28 ± 0.07	0.44 ± 0.13	>10
Re-54	0.73 ± 0.07	0.57 ± 0.05	0.23 ± 0.07
Re-66	0.66 ± 0.18	2.6 ± 0.4	3.8 ± 0.2

[a] Triplicate.
[b] Non-labeled equivalent of compound **T-7**.
[c] Previously reported IC_{50} was 0.086 μM [38].

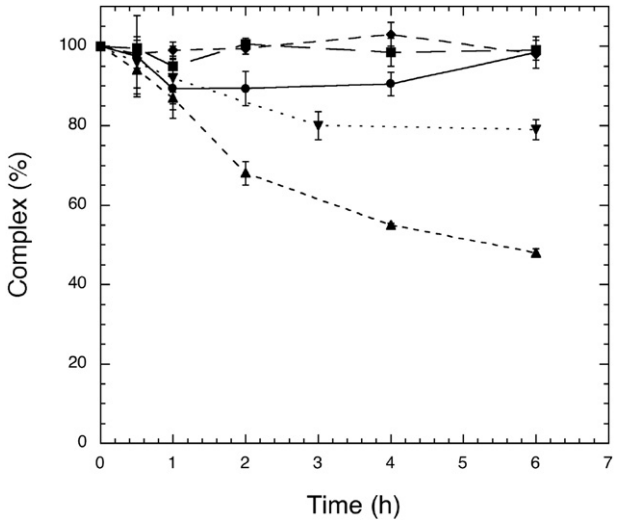

Fig. 4. Stability in a 35 mM HEPES buffer pH 7.8 at 20 °C of representative complexes in the presence of 1 mM glutathione: **Tc-16** (●, 2-aminoethanethiol C-term.), **Tc-24** (■, β-Ala at S2 and 2-aminoethanethiol C-term.), **Tc-38** (▲, 3-aminoethanethiol C-term.), **Tc-39** (▼, β-Ala at S2 and 3-aminoethanethiol C-term.) and **Tc-54** (◆, 3-aminothiophenol C-term.); **Tc-17** and **Tc-31** were not represented for clarity (curves are equivalent to that obtained for **Tc-24**).

glutathione (Fig. 4) [61,62]. However, C-terminus elongation seems to weaken Tc coordination by the NS_2/S chelation motif since only 50% of complex **Tc-38** was recovered after 6 h. Unexpectedly, concomitant introduction of a β-Ala residues and a 3-aminoethanethiol moiety does not amplify the deleterious effect of ring expansion since complex **Tc-39** exhibited a good stability (80% after 6 h).

Screening of all synthesized complexes towards the 3 integrins studied herein (Fig. 5) led to the selection of 4 new complexes **Re-33**, **Re-50**, **Re-54** and **Re-66** that bind to integrin αVβ3 with sub-micromolar affinities (Fig. 6, Table 2). However, none of them exhibits a higher affinity for αVβ3 or an apparent better selectivity than complex **Re-16** relative to integrins αIIbβ3 and αVβ5. No marked selectivity for a particular integrin was detected though tendencies can be drawn from the IC_{50} values. In example, complexes **Re-33** and **Re-50** seem to have a preference for integrins αVβ3 and αIIbβ3 relative to αVβ5. It is noteworthy that integrin αVβ3 seems to tolerate an inversion of absolute configuration at S1 (**Re-50** and **Re-66**) and also at S3 provided L-Asp is replaced with a D-Glu residue (**Re-33**). General rules cannot be drawn from these data, however, this result suggests that proper positioning of amino acid side-chains can compensate the effect of Cα inverse configuration to efficiently interact with the protein. Such a tolerance was not observed by Kessler and coworkers with cyclopentapeptides since inversion of configuration at the corresponding positions caused a dramatic fall of the affinity [54].

A satisfactory stability of the 4 new selected complexes in blood was assumed from our previous experience with **Tc-16**. However, in view of *in vivo* evaluation of these complexes in a murine tumor model, we studied the behavior of **Tc-33**, **Tc-50**, **Tc-54** and **Tc-66** in mice plasma (Fig. 7). The 2-aminoethanethiol-containing complex **Tc-33** exhibited a good stability that is comparable to that of its analog **Tc-16** [38] with more than 80% residual complex after 3 h. Conversely, complex **Tc-66** showed to be rather instable with about only 30% of the initial product remaining in solution after 3 h. Complexes **Tc-50** and **Tc-54** exhibited intermediary stabilities (50–70% after 3 h). In the case of complex **Tc-54**, dosage of radioactivity in both the precipitate and solution after removing plasma proteins by precipitation and centrifugation showed that the solution/protein-associated radioactivity was inverted from 65/35 (initial value) to 33/67 after 6 h. This result suggests that a decrease of complex concentration in solution might be related to an adsorption of tracers on plasma proteins. This adsorption might reflect a simple trapping of the tracer by circulating proteins though complex degradation by some thiol-rich plasma proteins such as serum albumin (whose Cys34 represents about 80% of plasma thiols) [63] and metallothionein [64] cannot be precluded. Conversely, other complexes evaluated gave mostly free technetium species (RP-HPLC $t_R = 3.9$ min) that were detected in solution and were not further identified.

At this point of the study, we decided to evaluate *in vivo* complexes **Tc-16**, **Tc-50** and **Tc-54** in nude mice (Balb/c *nu*/*nu*) bearing a human astrocytoma–glyoblastoma U87MG tumor xenograft that has been reported as overexpressing specifically integrin αVβ3. In this study, the rather instable complex **Tc-66** as well as complex **Tc-33** (which appeared as a mixture of 2 diastereomers) was also tested.

2.4. *In vivo* evaluation of tracers ***Tc-16***, ***Tc-33***, ***Tc-50***, ***Tc-54*** and ***Tc-66*** in mice

Preliminary studies using tracer **T-7** (obtained by simple propionylation of cyclopeptide **5** with tritiated propionyl-*N*-hydroxysuccinimide) showed that this compound specifically accumulated

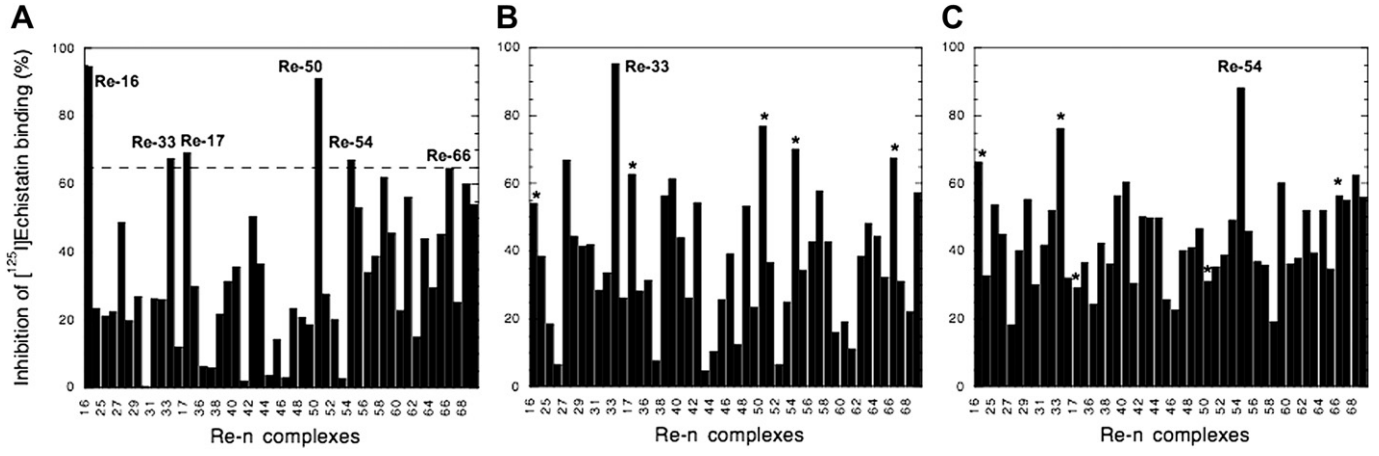

Fig. 5. Screening of 48 cyclic tracers **Re-16**, **Re-17** and **Re-24** to **Re-69** (1 μM) towards integrins αVβ3 (A), αIIbβ3 (B) and αVβ5 (C); bioactive compounds (inhibition > 65%) towards a given integrin are indicated with their product numbers and are marked with a star for other integrins; for integrin αVβ3 (A) the dotted line (65% inhibition at 1 μM) represents the limit of selection of active oxorhenium complexes; complexes order is presented according to Table 1.

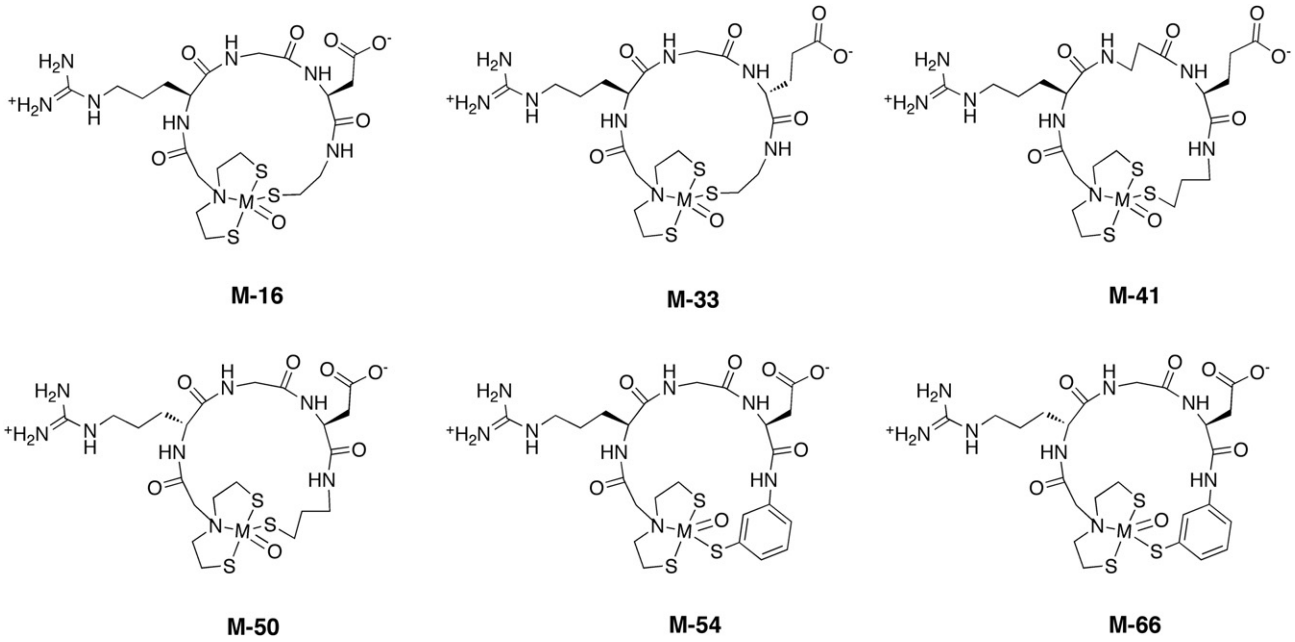

Fig. 6. ChemDraw structures of bioactive oxotechnetium (M is Tc) and oxorhenium (M is Re) **M-16**, **M-33**, **M-50**, **M-54** and **M-66**; the inactive complex **M-41** was also represented.

inside the tumor (ID/g 3.3%) since coinjection of an excess of non-radiolabeled peptides **3** or **7** caused an almost complete lack of accumulation of **T-7** (Table S4 in the Supplementary Material). We also evaluated the accumulation of both technetium gluconate and pertechnetate inside the tumor. $[^{99m}TcO(gluconate)_2]^-$ (or resulting reduced Tc species) did not accumulate significantly inside tumor U87MG (ID/g 0.06%). Conversely, a slight proportion (ID/g 0.28%) of $^{99m}TcO_4^-$ remained associated to the tumor 1 h after injection (0.31% after 3 h) (see Supplementary Material section).

We also studied the tissue repartition of the previously reported reference tracer **Tc-14** which was originally evaluated in mice bearing a human melanoma tumor M21 xenograft [27]. We observed that **Tc-14** accumulated also inside the U87MG tumor (ID/g 1.1%) that is reputed to overexpress αVβ3 integrin [17,24]. Moreover, coinjection of an excess of complex **Re-14** caused an almost total lack of accumulation of radioactivity at the tumor level. As reported by Haubner et al [27], **Tc-14** mainly accumulated inside the kidneys (see Supplementary Material section).

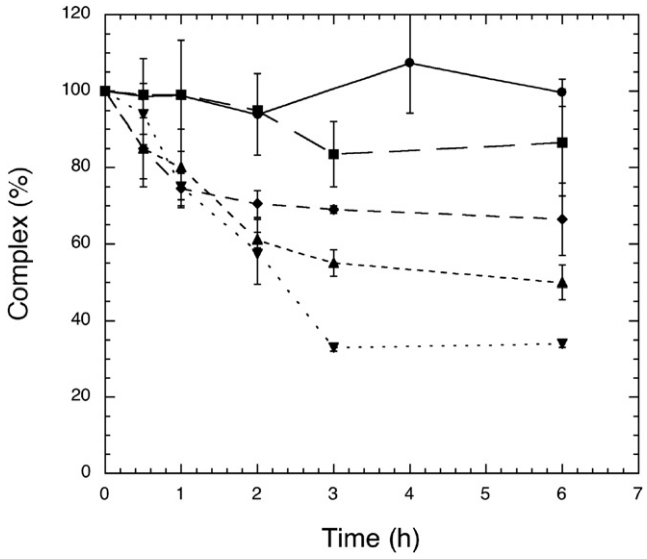

Fig. 7. Stability in mice plasma at 37 °C of complexes selected from the library: **Tc-16** (●), **Tc-33** (■), **Tc-50** (◆), **Tc-54** (▲) and **Tc-66** (▼); **Tc-33** appeared as a mixture of two major diastereomers.

Technetium complexes **Tc-16**, **Tc-33**, **Tc-50**, **Tc-54**, and **Tc-66** were injected as reported above and evaluated as new αVβ3 integrin-specific tracers. Compound **Tc-41** was also tested as a negative reference since it displayed no significant affinity *in vitro* for integrins αVβ3 and αIIbβ3 and a low affinity for integrin αVβ5. As expected, complexes **Tc-16** and **Tc-50** accumulated efficiently and sustainably inside the tumor (Table 3). Conversely, complexes **Tc-66** (instable in plasma) and **Tc-41** (inactive *in vitro*) displayed a background accumulation inside the tumor that was very similar to that of a non-specific tracer such as pertechnetate (ID/g 0.5%). Complexes **Tc-33** and **Tc-54** gave intermediary results with a satisfactory accumulation inside the tumor (not statistically different from **Tc-16** and **Tc-50**) but a high retention in spleen, kidneys and liver that suggests a rather slow excretion. In contrast, complexes **Tc-16** and **Tc-50** exhibited good ID/g in tumor (respectively 1.4 and 1.6% after 1 h, 1.2 and 1.3% after 3 h) along with relatively low accumulation in healthy tissues. Biodistribution studies showed that **Tc-50** has the lowest accumulation inside spleen, kidneys and liver in this series.

As already mentioned, complex **Tc-33** appeared to be formed as a 1:1 mixture of diastereomers. This result raises an interesting question: which of the two diastereomers is bioactive? To answer about this particular point, we had to separate the two oxorhenium isomers and to test them separately provided they do not interconvert spontaneously as already observed with compound **Re-16** [38]. However, we observed a fast isomerization that occurred at the experiment time-scale (about 2 h). The separation of diastereomers by RP-HPLC should even be more difficult with technetium complexes since it implies additional steps such as elimination of toxic acetonitrile, volume reduction and buffering that are not compatible with the timing of *in vivo* experiments. Therefore, complex **Tc-33** was not studied further.

Examination of ratios *T*/*B* and *T*/*M* (ratios of accumulation of radioactivity in tumor/blood and tumor/muscles, respectively) showed that compound **Tc-16** has a disappointing *T*/*B* relative to **Tc-14**, in particular after 1 h. A low *T*/*B* was also observed for complex

Table 3
Biodistribution (ID/g or mL%) 1 h /3 h after injection of specific radio-tracers in a model mice bearing a human U87MG xenograft.

Organ	**Tc-16**[b]	**Tc-33**[c]	**Tc-50**[b]	**Tc-54**[c]	**Tc-66**[c]	**Tc-14**[a] (reference)	**Tc-41**[a] (negative)
Blood	3.5 ± 1.2/1.4 ± 0.2	1.7 ± 0.4/0.8 ± 0.3	1.2 ± 0.7/2.9 ± 0.7	1.7 ± 0.1/1.4 ± 0.2	1.9 ± 0.2/1.0 ± 0.1	0.4/0.4	1.6/1.1
Spleen	1.9 ± 0.9/3.4 ± 1.4	5.7 ± 1.1/3.0 ± 0.7	0.4 ± 0.1/0.3 ± 0.1	3.5 ± 1.3/5.4 ± 1.3	20.8 ± 8.0/12.7 ± 0	1.4/1.3	0.7/0.2
Kidneys	6.3 ± 1.3/7.1 ± 3.3	2.8 ± 1.0/3.0 ± 0.9	5.9 ± 0.9/0.6 ± 0.1	6.4 ± 0.8/5.8 ± 1.4	3.1 ± 0.1/6.3 ± 3.6	28.0/25.7	9.7/6.5
Heart	0.8 ± 0.1/0.7 ± 0.1	0.8 ± 0.3/0.5 ± 0.2	0.8 ± 0.2/0.4 ± 0.1	0.8 ± 0.1/0.7 ± 0.1	0.7 ± 0/0.3 ± 01	0.6/0.7	0.7/0.5
Lungs	1.4 ± 0.2/1.1 ± 0.2	1.2 ± 0.4/1.0 ± 0.3	0.7 ± 0.3/0.7 ± 0.1	1.2 ± 0/1.0 ± 0.2	2.1 ± 0.4/1.0 ± 0.2	1.0/0.7	1.4/1.0
Liver	7.7 ± 3.1/10.8 ± 3.4	13.2 ± 1.6/18.4 ± 0.8	5.5 ± 0.9/4.8 ± 0.7	13.9 ± 0.8/16.1 ± 1.6	26.3 ± 12.0/7.0 ± 3.0	4.7/5.6	3.2/10.7
Pancreas	0.3 ± 0.1/0.2 ± 0	0.6 ± 0.2/0.5 ± 0.1	0.4 ± 0.1/0.3 ± 0.1	0.4 ± 0.1/0.2 ± 0.1	0.5 ± 0.2/0.1 ± 0	0.1/0.3	0.3/0.1
Muscles	0.3 ± 0.1/0.2 ± 0.1	0.5 ± 0.1/0.4 ± 0.2	0.5 ± 0.1/0.4 ± 0.1	0.3 ± 0.2/0.1 ± 0	0.5 ± 0.1/0.1 ± 0	0.2/0.2	ND/0.1
Tumor	1.4 ± 0.5/1.2 ± 0.1	1.3 ± 0.4/1.2 ± 0.3	1.6 ± 0.4/1.3 ± 0.1	1.2 ± 0.1/1.0 ± 0.2	0.5 ± 0.2/0.4 ± 0.2	1.1/1.0	0.4/0.5
T/*B*[d]	0.4/0.9	0.8/1.5	1.3/0.4	0.7/0.7	0.3/0.4	2.7/2.5	0.2/0.5
T/*M*[e]	4.7/6.0	2.6/3.0	3.2/3.2	4.0/10.0	1.0/4.0	5.5/5.0	−/5.0

[a] Monoplicate.
[b] Triplicate.
[c] Duplicate.
[d] Ratio tumor/blood.
[e] Ratio tumor muscles.

Tc-50 3 h after injection. These data might reflect a non-specific accumulation of radioactivity in blood vessels located at the periphery of highly vascularized tumors. However, this ratio strongly depends on the plasma levels of the injected complexes and therefore, a low *T*/*B* does not necessarily result from a lower efficacy of the tracer but might also reflect a higher stability of the oxorhenium chelate which might be slowly distributed in other tissues. To conclude about this point, we investigated the effect on radioactivity accumulation in tumor of the corresponding oxorhenium complexes on the one hand and of a known integrin antagonist on the other hand.

Coinjection of **Tc-16** or **Tc-50** with their respective rhenium equivalents **Re-16** or **Re-50** caused a significant fall of technetium accumulation inside the tumor (Fig. 8). This result suggests that tumor accumulation of radioactivity is saturable and is effectively related to an interaction of ^{99m}Tc-complexes at specific sites. Therefore, we can conclude that the apparent tumor concentration of tracers **Tc-16** and **Tc-50** does not result from a simple trapping of technetium in the tumor vascular network. We also observed that peptide **3**, a specific ligand of integrin αVβ3, competed with the tracers and strongly inhibited tumor uptake of complexes **Tc-16** and **Tc-50**. This competition unambiguously indicates that these tracers target integrin αVβ3 specifically in the tumor area. Conversely, rhenium analog **Re-41** that does not bind to integrin αVβ3 was unable to compete with the tracers **Tc-16** and **Tc-50** (Fig. 8). We checked that such a negative result could not arise from a possible instability of the complex. As expected, complex **Re-41** (as well as **Re-16** and **Re-50**) displayed satisfactory stabilities in mice plasma for at least 3 h.

3. Experimental protocols

3.1. General remarks

Chemical reagents and solvents were purchased from Sigma–Aldrich, VWR, Fluka or SDS and were of the highest purity available. Amino acids and resins were from Novabiochem. HATU was purchased from Molekula (UK). $[^{99m}TcO_4]^-$ was eluted as a physiological saline solution from commercially available ^{99}Mo/^{99m}Tc generator system (ELUMATIC III, CIS bio international). RP-HPLC purifications were achieved on a Prostar Varian chromatography system coupled to a Varian 335 diode array detector. RP-HPLC analysis were carried out either on a Varian Pursuit C18 column (analytical column 250 × 4.6 mm, 5 μm) protected by an analytical Security Guard (Phenomenex) or Waters 600/600E pumps coupled to a Waters 600 gradient controller and a Waters 996 diode array detector. RP-HPLC purifications were performed either on a Varian Pursuit C18 preparative column (250 × 21.2 mm, 5 μm) or on a Varian Pursuit C18 semi-preparative column (250 × 10.0 mm, 5 μm), eluted with various proportions of A and B (A: 0.1% aqueous solution of formic acid; B: 0.1% solution of formic acid in acetronitrile). The chromatography system was coupled to a gamma detector (radioflow monitor) HERM LB500 (Berthold). LC–MS analysis was carried out on an Agilent 1100 Series chromatography system, with a Varian Pursuit C18 analytical column, with a linear gradient system. The chromatography system was coupled to a Bruker Esquire HCT ES/MS mass spectrometers. ^{1}H and ^{13}C NMR spectra were recorded on Bruker AVANCE 250 and 400 NMR spectrometer; δ and *J* are reported in ppm relative to TMS and Hz, respectively. ES/MS analysis was carried out either on a Quattro Micro apparatus or on a Platform LCZ (Micromass). High-resolution mass spectrometry (HRMS) was performed on a Q-tof (Micromass).

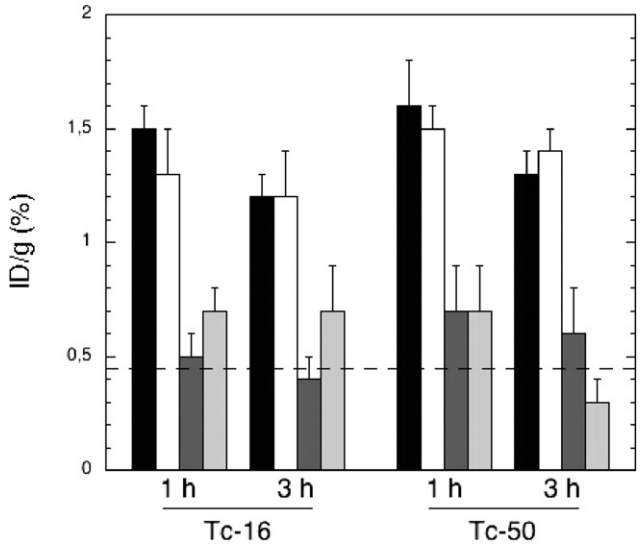

Fig. 8. ID/g (%) determined by tumor gamma-counting after competition experiments by coinjection of ^{99m}Tc tracers **Tc-16** or **Tc-50** with the corresponding Re-labeled compounds **Re-16** or **Re-50** (500 μg), integrin αVβ3 antagonist c(RGDyV) **3** (500 μg) and inactive complex **Re-41** in nude mice bearing U87MG human tumor xenografts: ^{99m}Tc tracer (black); ^{99m}Tc tracer + **Re-41** (white); ^{99m}Tc tracer + corresponding Re compound (grey); ^{99m}Tc tracer + compound **3** (light grey); the dotted line represents the average background radioactivity found in tumors by injection of a non-specific ^{99m}Tc-labeled compound (TcO_4^-).

Microplates were counted using a Perkin–Elemer microplate scintillation and luminescence counter Topcount NXT.

3.2. Chemistry

3.2.1. Peptide synthesis

Peptides were synthesized by standard Fmoc-solid phase peptide synthesis using either the commercially available cysteamine 4-methoxytrityl resin and 2-aminobenzenethiol 4-methoxytrityl resin (Novabiochem). The 3-aminopropanedisulfide group (see Supporting Material section) was prepared via a simple chemical route. The 4-aminothiophenol or 3-aminothiophenol motifs were grafted on to the Cl-Mmt resin using a standard procedure. Protecting groups used to mask the chemically reactive side-chains of amino acids were *t*Bu (Asp, Glu), Pbf (Arg) and ivDde (Dpr, Dab and Lys). Grafting of the first amino acid on to the linker was performed with HATU. Other coupling reactions were done using DCC/HOBT. The *N*-bis(2-thioethyl)glycine was synthesized as previously reported and coupled to the peptide N-terminus using HATU [47]. Peptides **18**–**23** were obtained by selective deprotection of side-chain aminogroups of the corresponding Dpr, Dab and Lys-containing peptides (ivDde protection) with 2% hydrazine monohydrate in DMF for 3 min. Their corresponding guanidinium equivalents were obtained by reaction with di-Boc-1H-pyrazole-1-carboxamidine (2.1 equiv.) in DMF overnight at room temperature. Peptides were cleaved and deprotected simultaneously using a mixture of TFA:TIPS:water 95:2.5:2.5 for 15 min at room temperature and were pre-purified by filtration though Sep-Pak cartridges using a gradient of 0.1% TFA in water to 0.1% TFA in acetonitrile. Purification by RP-HPLC was carried out using a semi-preparative column Varian Pursuit C18 (10 × 250 mm, 5 μm) at 5 mL min^{-1} with various linear gradients of 0.1% formic acid in water to 0.1% formic acid in acetonitrile in 30 min. Peptides were typically obtained with purities higher than 95% as assessed by analytical RP-HPLC elution (column Varian Pursuit C18 (4.6 × 250 mm, 5 μm) at 1 mL.min^{-1}) and LC–ES/MS analysis. All peptides isolated gave satisfactory high-resolution mass spectrometry analysis (error < 10 ppm).

3.2.2. Oxorhenium complexation (library/preparative)

Peptides (10 μmol/100 μmol) were dissolved in degassed methanol (150 μL/1.5 mL). A solution of tributylphosphine 10% in methanol (1.5 equiv.) was added and the mixture was stirred for 1 h at room temperature under argon. The solution was used immediately. Tetrabutylammonium tetrachlorooxorhenate (1 equiv.) in degassed methanol (150 μL/1.5 mL) and triethylamine (4 equiv.) were added to the solution of reduced peptide. The pH was adjusted to pH 10 with triethylamine. The mixture was stirred for 2 h at room temperature. The precipitate was isolated by repeated centrifugation/methanol washing cycles and purified by Sep-Pak filtration using a gradient of 0.1% TFA in water to 0.1% TFA in acetonitrile. Purity of the complexes was checked by LC–ES/MS analysis using a Varian Pursuit C18 column (4.6 × 250 mm, 5 μm) at 0.6 mL min^{-1} eluted with a linear gradient of A:B 85:15 to 70:30 in 30 min (A: 0.1% TFA in water; B: 0.1% TFA in acetonitrile). All complexes isolated displayed the canonic [NS_2·Re·S] isotopic motif and gave satisfactory high-resolution mass spectrometry analysis (error < 10 ppm). **Re-16**: LC–ES/MS: t_R 10.3 + 14.1 min, *m/z* 783.1 (purity 97%). HRMS: *m/z* calcd for $C_{20}H_{36}N_8O_7ReS_3$ 783.1427; found 783.1451. **Re-33**: LC–ES/MS: t_R 12.2 + 13.8 min, *m/z* 797.2 (purity 98%). HRMS: *m/z* calcd for $C_{21}H_{38}N_8O_7ReS_3$ 797.1583; found 797.1609. **Re-41**: LC–ES/MS: t_R 12.8 + 15.4 min, *m/z* 825.2 (purity 96%). HRMS: *m/z* calcd for $C_{24}H_{45}N_8O_7ReS_3$ 825.1896; found 840.2010. **Re-50**: LC–ES/MS: t_R 13.8 + 16.5 min, *m/z* 797.1 (purity 94%). HRMS: *m/z* calcd for $C_{21}H_{38}N_8O_7ReS_3$ 797.1583; found 797.1596. **Re-54**: LC–ES/MS: t_R 16.2 + 16.7 min, *m/z* 831.1 (purity 97%). HRMS: *m/z* calcd for $C_{24}H_{36}N_8O_7ReS_3$ 831.1427; found 831.1454. **Re-66**: LC–ES/MS: t_R 27.6 + 28.6 min, *m/z* 831.1 (purity 96%). HRMS: *m/z* calcd for $C_{24}H_{36}N_8O_7ReS_3$ 831.1427; found 831.1439.

3.2.3. Preparation of [^{99m}Tc]Technetium complexes

After reduction of the peptides (2 μmol) as described above, the solvent was removed under a flux of argon and the product was dissolved in a 35 mM HEPES buffer pH 7.8 to give a 500 μM solution of peptide. [^{99m}Tc]oxotechnetium gluconate was independently produced by mixing solutions of 2 mg mL^{-1} stannous chloride (2 μL) in HCl 0.1 N, 50 mM gluconate (10 μL), and a [^{99m}Tc]pertechnetate solution (90 μL, about 130 MBq) eluted from a ^{99}Mo/^{99m}Tc generator. The resulting [^{99m}Tc]oxotechnetium gluconate solution was treated for 15 min at 90 °C with the solution of reduced peptide (100 μL). Complexes purities were evaluated by radio-RP-HPLC (analytical column Varian Pursuit C18 4.6 × 250 mm, 5 μm) connected to a gamma counter at 1 mL min^{-1} using a linear gradient system A:B 85:15 to 70:30 in 30 min (A: 0.1% formic acid in water; B: 0.1% formic acid in acetonitrile). **Tc-16**: t_R = 15.1 min (98%), **Tc-17**: t_R = 14.6 min (95%), **Tc-24**: t_R = 15.9 min (99%), **Tc-31**: t_R = 14.7 min (95%), **Tc-33**: t_R = 13.5 + 14.9 min (86%), **Tc-38**: t_R = 18.7 min (96%), **Tc-39**: t_R = 22.1 min (95%), **Tc-41**: t_R = 21.8 min (93%), **Tc-50**: t_R = 18.3 min (98%), **Tc-54**: t_R = 35.8 min (95%), **Tc-66**: t_R = 33.3 min (94%).

Reference complex **Tc-14** was prepared as previously reported [27].

3.2.4. Stability of complexes *Re-16*, *Re-41* and *Re-50* in murine plasma

A 20 mM solution of oxorhenium complex in DMSO (15 μL) was added to fresly prepared murine plasma (135 μL) and the mixture was incubated at 37 °C for 3 h. After precipitation of plasma proteins with methanol (90 μL) and centrifugation (1 min at 7.2 g), the solution was analyzed by LC–ES/MS using a reverse phase column (Waters Atlantis dC18 3 mm, 4.6 × 150 mm, 90 Å) eluted with a linear gradient (A–B: 15–30% in 30 min; A: 0.1% formic acid in water, B: 0.1% formic acid in acetonitrile; 0.6 mL min^{-1}): **Re-16**, t_R = 10.2 + 14.0 min (*m/z* 783.1); **Re-41**, t_R = 12.6 + 15.3 min (m/z 825.1); **Re-50**, t_R = 13.7 + 16.6 min (*m/z* 797.1).

3.2.5. Stability of [^{99m}Tc]Technetium complexes in murine plasma

A solution of complex (25 μL, typically 20–40 MBq) was added to freshly prepared murine plasma (125 μL) and the mixture was incubated at 37 °C. Aliquots (10 μL) were isolated after 0, 0.5, 1, 2, 4 and 6 h. Proteins were precipitated with methanol (90 μL) and eliminated by centrifugation. The supernatant was analyzed by analytical radio-RP-HPLC (same gradient as above).

3.2.6. Resistance of [^{99m}Tc]Technetium complexes to GSH

A solution of complex (200 μL, 50–100 MBq) was added to a degassed HEPES buffer (25 μL, 35 mM, pH 7.8) followed by a 10 mM solution of GSH in HEPES buffer (25 μL). The mixture was incubated at room temperature. Aliquots (10 μL) were diluted in water (990 μL) after 0, 0.5, 1, 2, 4 and 6 h and were analyzed by analytical radio-RP-HPLC as described above.

3.3. Biology

3.3.1. Integrin binding assays

αVβ3 and αVβ5 integrin receptors (Millipore) and αIIbβ3 integrin receptors (Enzyme Research, Swansea, UK) were diluted at 1000 ng/ml in coating buffer (20 mM Tris HCl pH 7.4, 150 mM NaCl, 2 mM $CaCl_2$, 1 mM $MgCl_2$, 1 mM $MnCl_2$) and aliquots of 100 μl/well were added to a 96-well plates (Millipore, Multiscreen-IP HTS) and incubated overnight at 4 °C. The plate was washed with the blocking/

binding buffer (50 mM Tris HCl pH 7.4, 100 mM NaCl, 2 mM $CaCl_2$, 1 mM $MgCl_2$, 1 mM $MnCl_2$) and Bovine Serum Albumin (1% for αVβ3 and αVβ5 or 5% for αIIbβ3), and incubated for an additional 2 h at room temperature. Then the plate was incubated in the presence of varying amounts of competing ligand (0.1 nM–10 μM RGD peptide **2** or **7**, or oxorhenium complex) for 3 h with [^{125}I]I-echistatin (0.06 nM for αVβ3 and αIIbβ3 or 0.1 nM for αVβ5). After incubation wells were washed two times with the blocking/binding buffer and counted by liquid scintillation method. Library screening was carried out for 2 concentrations in oxorhenium complexes (1 and 10 μM in monoplicate). For IC_{50} determination, each data point is the result of the average of triplicate wells.

3.3.2. U87MG cell culture and tumor xenografts

U87MG cells (ETCC) were grown at 37 °C under a 5% CO_2 atmosphere in the Eagle's Minimum Essential Medium (EMEM, 500 mL) complemented with 2 mM glutamine, 1% non-essential amino acids (commercial cocktail), 1 mM sodium pyruvate, 10% v/v of fetal calf serum with penicillin (100 U mL^{-1}) and streptomycin (100 μg mL^{-1}). Tumors were obtained by subcutaneous injection of about 5×10^6 cells suspended in EMEM (150 μL) to the right shoulders of female athymic nude mice (Balb/c *nu*/*nu*) obtained from Charles River Lab. (Lyon, France) at 7 weeks of age (~20 g). When the tumors reach 2–4 mm in diameter, the mice were used for biodistribution studies according a protocol that has been approved by the French Animal Care and Use Committee (Décret 87-848, 87-10-19). Animals were anesthetized with 2% isoflurane.

3.3.3. Biodistribution studies

Typically 25–50 MBq of tracer were injected to each mouse bearing a U87MG tumor. The animals were sacrificed by exsanguination and dissected 60 or 180 min after injection. The organs of interest and tumors were removed, weighted and the radioactivity in the tissues was measured using a gamma counter. Results are expressed as the percentage of the injected dose per gram of tissue (%ID/g). Typically, each value represents the mean ± standard deviation (SD) of 2–5 animals.

4. Conclusions

We described the design and synthesis of cyclic oxorhenium and oxotechnetium complexes that mimic a RGD sequence, and their *in vitro* and *in vivo* evaluations as specific ligands of integrin αVβ3. Among the 55 complexes tested, 6 were identified as antagonists of integrin αVβ3 with 2 of them (**Re-33** and **Re-54**) binding preferentially to integrins αIIbβ3 and αVβ5, respectively. Five oxorhenium complexes (**Re-16**, **Re-33**, **Re-50**, **Re-54** and **Re-66**) were selected for *in vivo* evaluation in mice bearing a human tumor model xenograft. *In vivo* experiments using the ^{99m}Tc-labeled equivalents of bioactive oxorhenium complexes showed that complexes **Tc-16** and **Tc-50** exhibit the most interesting properties for tumor imaging in mouse with ID/g of, respectively, 1.4 and 1.6% after 1 h and a limited accumulation in healthy tissues. Using competition experiments, we showed that complexes **Tc-16** and **Tc-50** specifically target integrin αVβ3 and are suitable for the molecular imaging of tumors. Although complex **Re-50** exhibits an IC_{50} for integrin αVβ3 which is significantly higher than that of **Re-16**, the corresponding tracer **Tc-50** seems to be more efficacious in particular due to a more selective targeting of tumor relative to other organs. We demonstrated that the 17-membered Tc-cyclized peptides **Tc-16** and **Tc-50** are attractive templates for development of new integrin-specific tracers usable for the molecular imaging of cancer. Improvement of affinity, selectivity and tumor targeting (versus healthy tissues) should be obtained by replacement of the arginine side-chain with non-guanidinium mimetics and aspartate mimetics that have been described in the literature. This approach should be facilitated by the development of a more versatile combinatorial synthetic strategy in order to access to larger sets of peptides.

Acknowledgements

We gratefully acknowledge the INCa (Institut National du Cancer) for the financial support of this work (grant # PL_06_060). We thank Steven Dubois (iBiTec-S/SIMOPRO) for LC–ES/MS analysis and Dr. Elisabeth Zeckri for help in 400 MHz NMR experiments. We are indebted to Dr. Carole Fruchart for echistatin iodination and to Dr. Denis Servent for technical assistance and helpful discussion during binding experiments.

Appendix A. Supplementary information

Supplementary information associated with this article can be found, in the online version, at doi:10.1016/j.ejmech.2011.02.032.

References

[1] F.M. Watt, EMBO J. 21 (2002) 3919–3926.
[2] B. Wehrle-Haller, B.A. Imhof, J. Pathol. 200 (2003) 481–487.
[3] S.A. Mousa, Mol. Biotechnol. 38 (2008) 33–40.
[4] W. Guo, F.G. Giancotti, Nat. Rev. Mol. Cell Biol. 5 (2004) 816–826.
[5] G. Bergers, D. Hanahan, Nat. Rev. Cancer 8 (2008) 592–603.
[6] E. K-Gottschalk, H. Kessler, Angew. Chem. Int. Ed. 41 (2002) 3767–3774.
[7] J.D. Humphries, A. Byron, M.J. Humphries, J. Cell Sci. 119 (2006) 3901–3903.
[8] D. Heckmann, B. Laufer, L. Marinelli, V. Limongelli, E. Novellino, G. Zahn, R. Stragies, H. Kessler, Angew. Chem. Int. Ed. 48 (2009) 4436–4440.
[9] B. Cacciari, G. Spalluto, Curr. Med. Chem. 12 (2005) 51–70.
[10] J. Chatterjee, O. Ovadia, G. Zahn, L. Marinelli, A. Hoffman, C. Gilon, H. Kessler, J. Med. Chem. 50 (2007) 5878–5881.
[11] M. Schotellius, B. Laufer, H. Kessler, H.-J. Wester, Acc. Chem. Res. 42 (2009) 969–980.
[12] S. Liu, Bioconjugate Chem. 20 (2009) 2199–2213.
[13] S. Liu, Mol. Pharm. 3 (2006) 472–487.
[14] W. Cai, S.S. Gambhir, X. Chen, BioTechniques 6 (2005) 6–17.
[15] M.R. Lewis, J. Nucl. Med. 46 (2005) 2–4.
[16] R. Haubner, H.-J. Wester, U. Reuning, R. Senekowitsch-Schmidtke, B. Diefenbach, H. Kessler, G. Stöcklin, M.J. Schwaiger, Nucl. Med 40 (1999) 1061–1071.
[17] X. Zhang, Z. Xiong, Y. Wu, W. Cai, J.R. Tseng, S.S. Gambhir, X. Chen, J. Nucl. Med. 47 (2006) 113–121.
[18] R. Haubner, W.A. Weber, A.J. Beer, E. Valbuliene, D. Reim, M. Sarbia, K.-F. Becker, M. Goebel, R. Hein, H.-J. Wester, H. Kessler, M. Schwaiger, PLOS Med. 2 (2005) 244–252.
[19] R. Haubner, B. Kuhnast, C. Mang, W.A. Weber, H. Kessler, H.-J. Wester, M. Schwaiger, Bioconjugate Chem. 15 (2004) 61–69.
[20] X. Chen, R. Park, M. Thome, A.H. Shahinian, J.R. Bading, P.S. Conti, Bioconjugate Chem. 15 (2004) 41–49.
[21] X. Chen, R. Park, Y. Hou, V. Khankaldyyan, I. Gonzales-Gomez, M. Thome, J.R. Bading, W.E. Laug, P.S. Conti, Eur. J. Nucl. Med. Mol. Imaging 31 (2004) 1081–1089.
[22] X. Chen, R. Park, A.H. Shahinian, M. Thome, V. Khankaldyyan, M.H. Bozorgzahed, J.R. Bading, R. Moats, W.E. Laug, P.S. Conti, Nucl. Med. Biol. 31 (2004) 179–189.
[23] Y. Wu, X. Zhang, Z. Xiong, Z. Cheng, D.R. Fischer, S. Liu, S.S. Gambhir, X. Chen, J. Nucl. Med. 46 (2005) 1707–1718.
[24] X. Chen, Y. Hou, M. Thome, R. Park, V. Khankaldyyan, I. Gonzales-Gomez, J.R. Bading, W.E. Laug, P.S. Conti, J. Nucl. Med. 45 (2004) 1776–1783.
[25] S. Alves, J.D.G. Correia, L. Gano, T.L. Rold, A. Prasanphanich, R. Haubner, M. Rupprich, R. Alberto, C. Dechristoforo, I. Santos, C.J. Smith, Bioconjugate Chem. 18 (2007) 530–537.
[26] R. Haubner, F. Bruchertseifer, M. Bock, H. Kessler, M. Schwaiger, H.-J. Wester, Nuklearmedizin 43 (2004) 26–32.
[27] S. Liu, D.S. Edwards, A.R. Harris, Bioconjugate Chem. 9 (1998) 583–595.
[28] F. Z-Su, G. Liu, S. Gupta, Z. Zhu, M. Rusckowski, D.J. Hnatowich, Bioconjugate Chem. 13 (2002) 561–570.
[29] F. Z-Su, J. He, M. Rusckowski, D.J. Hnatowitch, Nucl. Med. Biol. 30 (2003) 141–149.
[30] B. Jia, J. Shi, Z. Yang, B. Xu, Z. Liu, H. Zhao, S. Liu, F. Wang, Bioconjugate Chem. 17 (2006) 1069–1076.
[31] S. Liu, W.-Y. Hsieh, Y. Jiang, Y.-S. Kim, S.G. Sreerama, X. Chen, B. Jia, F. Wang, Bioconjugate Chem. 18 (2007) 438–446.
[32] M.L. Janssen, W.J. Oyen, I. Dijkgraaf, L.F. Massuger, C. Frielink, D.S. Edwards, M. Rajopadhye, H. Boonstra, F.H. Corstens, O.C. Boerman, Cancer Res. 62 (2002) 6146–6151.

[33] B.H. Kujipers, S. Groothuys, A.C. Soede, P. Laverman, O.C. Boerman, F.L. van Delft, F.P.J.T. Rutjes, Bioconjugate Chem. 18 (2007) 1847–1854.
[34] X. Chen, R. Park, A.H. Shahinian, J.R. Bading, P.S. Conti, Nucl. Med. Biol. 31 (2004) 11–19.
[35] R. Haubner, H.-J. Wester, F. Burkhart, R. Senekowitsch-Schmidtke, W. Weber, S.L. Goodman, H. Kessler, M. Schwaiger, J. Nucl. Med. 42 (2001) 326–336.
[36] J. Zeng, W.-H. Xie, S.-L. Hu, M.-X. Jin, Chinese Med. J. 119 (2006) 1435–1443.
[37] Y. Shi, S. Sharma, Bioorg. Med. Chem. Lett. 9 (1999) 1469–1474.
[38] M. Aufort, M. Gonera, N. Chaignon, L. Le Clainche, C. Dugave, Eur. J. Med. Chem. 44 (2009) 3394–3401.
[39] M.F. Giblin, N. Wang, T.J. Hoffman, S.S. Jurisson, T.P. Quinn, Proc. Natl. Acad. Sci. U. S. A. 95 (1998) 12814–12818.
[40] M.F. Giblin, S.S. Jurisson, T.P. Quinn, Bioconjugate Chem. 8 (1997) 347–353.
[41] Z. Cheng, J. Chen, Y. Miao, N.K. Owen, T.P. Quinn, S.S. Jurisson, J. Med. Chem. 45 (2002) 3048–3056.
[42] Y. Barda, N. Cohen, V. Lev, N. Ben-Aroya, Y. Koch, E. Mishani, M. Fridkin, C. Gilon, Nucl. Med. Biol. 31 (2004) 921–933.
[43] H.M. Bigott-Hennkens, S. Junnotula, L. Ma, F. Gallazzi, M.R. Lewis, S.S. Jurisson, J. Med. Chem. 51 (2008) 1223–1230.
[44] G. Fridkin, T.A. Bonasera, P. Litman, C. Gilon, Nucl. Med. Biol. 32 (2005) 39–50.
[45] Y. Fu, M. Létourneau, Q.T. Nguyen, D. Chatenet, J. Dupuis, A. Fournier, Eur. J. Pharmacol. 617 (2009) 118–123.
[46] B. Costopoulos, D. Benaki, M. Pelecanou, E. Mikros, C.I. Stassinopoulou, A.D. Varvarigou, S.C. Archimandritis, Inorg. Chem. 43 (2004) 5598–5602.
[47] C. Clavaud, M. Heckenroth, C. Stricane, A. Menez, C. Dugave, Bioconjugate Chem. 17 (2006) 807–814.
[48] Z. Su, Y. Xu, J. Label Compd. Radiopharm. 51 (2008) 93–100.
[49] C. Clavaud, J. Le Gal, R. Thai, M. Moutiez, C. Dugave, ChemBioChem 9 (2008) 1823–1829.
[50] J.E. Cyr, D.A. Pearson, C.A. Nelson, B.A. Lyons, Y. Zheng, J. Bartis, J. He, M.V. Cantorias, R.C. Howell, J. Med. Chem. 50 (2007) 4295–4303.
[51] C. Clavaud, M. Heckenroth, C. Stricane, M.-A. Lelait, A. Menez, C. Dugave, ChemBioChem 7 (2006) 1352–1355.
[52] R. Dayam, F. Aiello, J. Deng, Y. Wu, A. Garofalo, X. Chen, N. Neamati, J. Med. Chem. 49 (2006) 4526–4534.
[53] L. Marinelli, A. Lavecchia, E. K-Gottschalk, E. Novellino, H. Kessler, J. Med. Chem. 46 (2003) 4393–4404.
[54] R Haubner D Finsinger H Kessler Angew Chem Int Ed Engl 36 (1997) 1374–1379.
[55] W. Chan, P. White, Fmoc Solid Phase Peptide Synthesis. Oxford University Press, New York, 2000.
[56] Y. Yang, W.S. Sweeney, K. Schneider, S. Thörnqvist, B.T. Chait, J.P. Tam, Tetrahedron Lett. 35 (1994) 9689–9692.
[57] E. Nicolas, E. Pedroso, E. Giralt, Tetrahedron Lett. 30 (1989) 497–500.
[58] J. Zhu, R.E. Marchant, J. Pept. Sci. 14 (2007) 690–696.
[59] R.S. Feinberg, R.B. Merrifiel, J. Am. Chem. Soc. 97 (1975) 3485–3496.
[60] K. Schwochau, Technetium: Chemistry and Radiopharmaceutical Applications. Wiley-VCH, 2000.
[61] X. Wang, Z. Guo, Anti-cancer Agents Med. Chem. 7 (2007) 19–34.
[62] D.M. Townsend, K.D. Tew, H. Tapiero, Biomed. Pharmacother. 47 (2003) 145–155.
[63] P.J. Sadler, Z. Guo, Pure Appl. Chem. 70 (1998) 863–871.
[64] J.S. Lazo, S.M. Kuo, E.S. Woo, B.R. Pitt, Chem.Biol. Interact. 111–112 (1998) 255–262.